Journal of Ship Research, Vol. 53, No. 3, September 2009, pp. 121–129

Journal of
Ship Research

Optimal Short-Range Routing of Vessels in a Seaway

I. S. Dolinskaya,* **M. Kotinis,†** **M. G. Parsons,‡** and **R. L. Smith***

**Department of Industrial and Operations Engineering, University of Michigan, Ann Arbor, Michigan*
†*Department of Mechanical Engineering, Old Dominion University, Norfolk, Virginia*
‡*Department of Naval Architecture and Marine Engineering, University of Michigan, Ann Arbor, Michigan*

An investigation of the optimal short-range routing of a vessel in a stationary random seaway is presented. The calculations are performed not only in head seas but also in oblique waves. The evaluation of the added drag is performed by computing the time average wave force acting on the vessel in the longitudinal direction. Subsequently, the added drag is superimposed on the steady drag experienced by the ship as it advances in calm water. In this manner, the fastest path between the origin point *A* and the destination point *B* can be evaluated, taking into account operational constraints. To obtain the fastest path between two points, the underlying structure and properties of the maximum mean attainable speed are analyzed. This detailed analysis allows us to demonstrate the fastest path for the problem without any operational constraints to be a straight line. Subsequently, the solution is reevaluated for scenarios where the original optimal path violates at least one of the operability criteria considered. For that case, a fastest path is found to be a path consisting of one waypoint, that is, a two line segment path. In addition to providing a closed-form fastest-path solution for the case of no operational constraints, a bound is provided for travel time error for more general speed functions in the case where a straight line path is followed.

Keywords: maneuvering; sea keeping; ship motions; operations (general)

1. Introduction

VARIOUS ADDED resistance computation methods have been proposed over the years; among these, the methods of Maruo (1957), Salvesen (1978), Lin and Reed (1976), and Gerritsma and Beukelman (1964, 1972) have been widely used. A thorough comparison between experimental and theoretical results can be found in the paper by Strom-Tejsen et al. (1973). The method developed by Salvesen is used here since it has been shown to provide reliable results over a wide range of vessel types with different hull forms and transom stern shapes. Salvesen's method is applicable not only to head seas but also to oblique waves.

The added resistance in regular waves is expressed as a product of first-order terms, using results obtained from ship motion analysis. The latter has been performed using the linear ship-motion strip theory (Salvesen et al. 1970). The added resistance in an irregular seaway is evaluated using the principle of superposition, which has been shown to be applicable to seakeeping problems (St. Denis & Pierson 1953). In long-crested seas, the mean added resistance can be computed by the formula:

$$\overline{R}(V,\theta) = 2\int_0^\infty R_{\mathrm{AW}}(V,\theta,\omega)\cdot S(\omega)d\omega \qquad (1)$$

where R_{AW} is the added resistance in regular waves, V is the vessel speed, ω is the wave frequency, θ is the ship heading angle relative to the wave direction, and $S(\omega)$ is the energy spectral density.

The computations for this research were performed using the methods described in this section, which are implemented in the commercial seakeeping analysis software program Seakeeper (FDS 2006a). Seakeeper is part of the ship design software suite Maxsurf (FDS 2006b), which was also employed to model the hull of the S-175 container ship used in the current investigation. While fastest-path finding is more relevant for navy and rescue vessels, the analysis here is for a container ship since the S-175 is a standard

Manuscript received at SNAME headquarters November 1, 2007; revised manuscript received September 26, 2008.

vessel used in naval research, and it has the most complete set of specifications and analysis results available to the public.

The seaway is simulated by a wave energy spectrum. In the current analysis, the International Ship and Offshore Structures Congress (ISSC) spectrum was used, as it is considered representative of a fully developed sea in open-sea conditions. The use of the ISSC spectrum requires the input of two parameters, namely, the significant wave height H_s and the characteristic wave period, T_1. Both parameters depend on the sea conditions the vessel is expected to encounter in a specific seaway. Typical sea state conditions, representative of the North Atlantic and North Pacific oceans, can be found in Lee et al. (1985). These values were implemented in the current investigation.

Constraints were introduced in the computational procedure by evaluating typical operability limiting criteria for each sea state and ship heading. The probability of slamming, the probability of deck wetness, the root mean square (RMS) roll value, and the RMS vertical acceleration values at the vessel's forward perpendicular (FP) and at the bridge comprise typical operability limiting criteria for merchant vessels (NORDFORSK 1987).

The fastest-path finding problem has been previously discussed for optimal yacht sailing and vessel routing subjected to weather effects. Philpott et al. (1993) created a yacht velocity prediction program and then used the program's results in dynamic programming algorithms to approximate the optimal paths. Their problem addresses longer-range trips where time and space homogeneity, assumed here, could not be exploited, resulting in an approximation algorithm.

Another group of researchers used the calculus of variations and optimal control theory to find an optimal vessel route. Faulkner (1963) and Papadakis and Perakis (1990) used Euler's equations to characterize an optimal path, which resulted in a system of differential equations that need to be solved in order to find the fastest path. Unlike previously published work, the underlying structure of the speed functions is explored here, and this provides closed-form and easy-to-compute solutions to optimal vessel routing. It is also worth noting that some researchers exploit the analogy between the refraction of light and fastest paths in their work (Mitchell & Papadimitriou 1991); however, this equivalence cannot be applied to our problem since we assume space homogeneity of the medium.

2. Methodology

The added resistance of the S-175 container ship in irregular waves was computed for various sea states and vessel headings. The hull surface was generated in Maxsurf and analyzed in Seakeeper. The main particulars of this vessel are demonstrated in Table 1. The service speed is set at 11.4 m/s, which corresponds to a Froude number, $Fn = 0.275$. Experimental data regarding measurements of added resistance in regular waves are available in the literature (Fujii & Takahashi 1975, Nakamura 1976).

Table 1 Main particulars of the S-175 container ship

Length between perpendiculars (m)	175.0
Breadth molded (m)	25.4
Design draft (m)	9.5
Freeboard (m)	7.0
Displacement (tonnes)	24,272

The computations were performed for Sea States 3 through 7. The probability of occurrence of the aforementioned sea states in the North Atlantic and North Pacific oceans is provided in Table 2. The operability limiting criteria assumed for the S-175 container ship are listed in Table 3.

The calm-water resistance of the S-175 container ship was computed using the commercial ship resistance evaluation software program Hullspeed (FDS 2006c), which is part of the ship design software suite Maxsurf. The resistance evaluation follows the method proposed by Holtrop (1984). The seakeeping analysis was performed in Seakeeper by dividing the vessel into 51 equally spaced stations along its length and using 11 conformal mapping terms. The analysis was performed for 91 frequency values to obtain smooth curves for the response amplitude operators (RAOs).

2.1. Computation of maximum mean attainable speed and operational constraints

The mean added resistance for various sea states and vessel headings was computed at different ship speeds, including the ship service speed. The resulting added resistance curve was then superposed on the calm-water resistance curve to produce the new propeller-load curve. The intersection between the propeller-load curve and the engine-power curve, assuming diesel propulsion within the service margin allowance giving a fixed engine rpm condition, yields to the maximum mean attainable vessel speed for the given sea state and ship heading. An inherent assumption in this procedure is that the engine is considered to be rpm limited; that is, a suitably large service margin has been included.

The RMS vertical acceleration at the bridge was computed at a point 30% L_{BP} aft of amidships, 50% of the ship depth above the main deck and on the centerline. The RMS vertical acceleration at the FP was computed at a point located on the main deck and on the centerline. The probabilities of slamming and deck wetness were computed assuming that the probability density function of the vessel motions follows a Rayleigh distribution. The probability of slamming was computed at a point 5% L_{BP} aft of the FP on the centerline and on the baseline using (Ochi & Motter 1973):

Table 2 Sea state occurrences in the North Atlantic and North Pacific

	Probability of Occurrence	
Sea State	North Atlantic	North Pacific
3	23.70	15.50
4	27.80	31.60
5	20.64	20.94
6	13.15	15.03
7	6.05	7.00

Table 3 Operability criteria values for S-175 container ship

Probability of slamming	0.023
Probability of deck wetness	0.050
RMS vertical acceleration at bridge (m/s^2)	1.472
RMS vertical acceleration at FP (m/s^2)	1.978
RMS roll (deg)	6.0

$$P(\text{slam}) = \exp\left(\frac{-T^2}{2m_{0zr}} + \frac{-v_{cr}^2}{2m_{0\dot{z}r}}\right) \quad (2)$$

where T is the draft of the vessel at a station 45% of the vessel length forward of the midship section, and m_{0zr} and $m_{0\dot{z}r}$ are the mean square relative vertical motion and velocity at the aforementioned station, respectively.

The critical or threshold velocity, v_{cr}, was computed using Froude scaling and an empirical estimate by Ochi and Motter (1973):

$$v_{cr} = 0.0928 \cdot \sqrt{gL_{BP}} \quad (3)$$

where g is the gravity constant.

The probability of deck wetness was computed using:

$$P(\text{deck wetness}) = \exp\left(\frac{-F^2}{2m_{0zr}}\right) \quad (4)$$

where F is the freeboard and m_{0zr} is the mean square relative vertical motion at a station 25% of the vessel length forward of the midship section.

The roll motion of the vessel was analyzed using the software program SEAKEEP.NTD (Beck et al. 2004) to obtain the RMS roll values. This program also uses the linear ship-motion strip theory (Salvesen et al. 1970) to calculate the ship motions in the frequency domain. However, it utilizes Frank's (1967) close-fit source distribution method, instead of conformal mapping, for the calculation of the hydrodynamic properties of the hull sections. The roll damping coefficient was set to a value of 0.08. Other computational parameters were set at the values used in Seakeeper.

3. Numerical results

The computed results of the seakeeping model provide the maximum mean attainable vessel speed for each given sea state and ship heading. The vessel speed was calculated for relative heading directions in the range from 0° (following seas) to 180° (head seas) relative to the dominant wave direction in increments of 15°. The maximum mean attainable speed at different ship headings for Sea States 3 through 7 is plotted in Fig. 1. Voluntary speed loss is not included.

In Sea States 6 and 7, the maximum involuntary speed loss occurs around a heading angle of 105°. This result can be explained by observing plots of the vessel heave and pitch RAOs for Fn = 0.275 in Figs. 2 and 3, respectively, as well as equation (1). The energy content of the ISSC spectrum is contained in a limited range of wave lengths. The fact that the motions' peak value shifts to shorter wave lengths with decreasing heading angle, results in larger integral values calculated through equation (1). In beam seas, even though the pitch motion is negligible, the substantial heave motion, especially at short wave lengths, leads to considerable mean added resistance values.

Given that the motion peaks occur at shorter wave lengths for quartering, beam, and following seas, the assumption of a slender body used in the derivation of both the ship motion strip theory and the added resistance theory is less valid. Therefore, the computed values are expected to have less accuracy for ship heading angles away from the vicinity of 180°. Compared with experimental data in head seas (ITTC 1987), the heave RAO

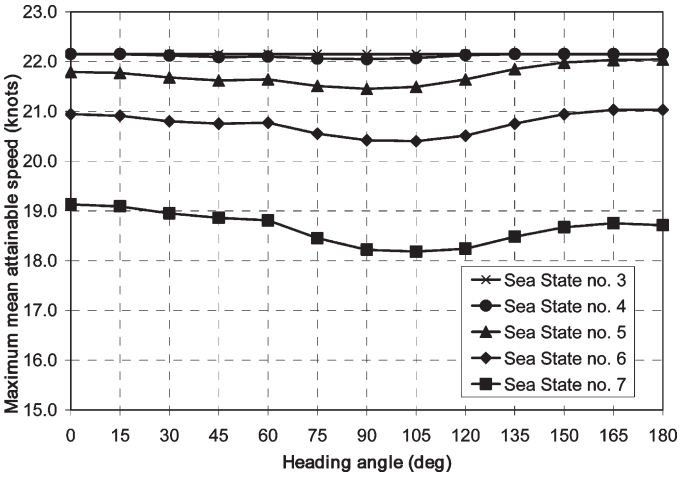

Fig. 1 Maximum mean attainable speed for S-175 as a function of ship relative heading angle and sea state

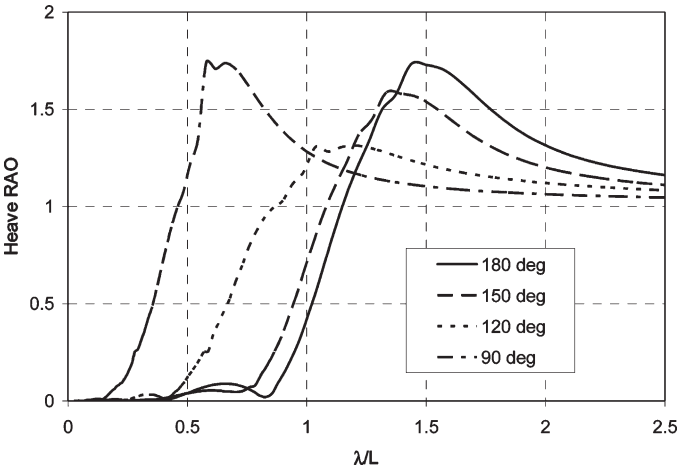

Fig. 2 Heave RAO at Fn = 0.275 for S-175 as a function of ship relative heading angle

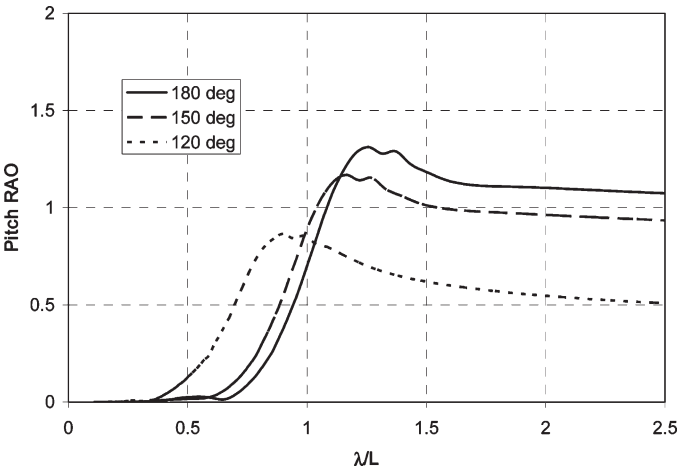

Fig. 3 Pitch RAO at Fn = 0.275 for S-175 as a function of ship relative heading angle

peak is overpredicted, but the pitch RAO is predicted quite accurately.

The RMS roll values are displayed in Fig. 4. The peak values at any sea state occur at a ship relative heading angle of 60°. The computed values for the probabilities of slamming and deck wetness are displayed in Figs. 5 and 6, respectively. For Sea States 3 through 5, the probabilities of slamming and deck wetness are zero; thus, they are not depicted in the corresponding figures. The RMS vertical acceleration values at the bridge and the FP are displayed in Figs. 7 and 8, respectively.

4. Optimal path

In severe sea states, the vessel operation is mostly limited by the ship motions relative to operational constraints rather than added resistance. Therefore, both effects were investigated: involuntary speed loss caused by added resistance and the limitations imposed by operational constraints.

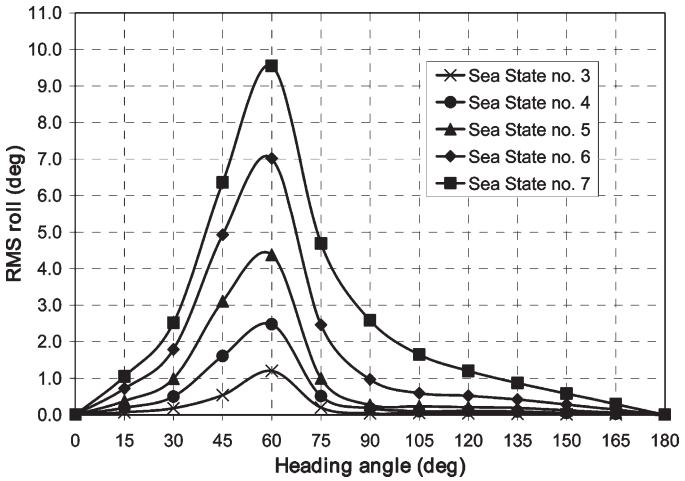

Fig. 4 RMS roll for S-175 as a function of ship relative heading angle and sea state

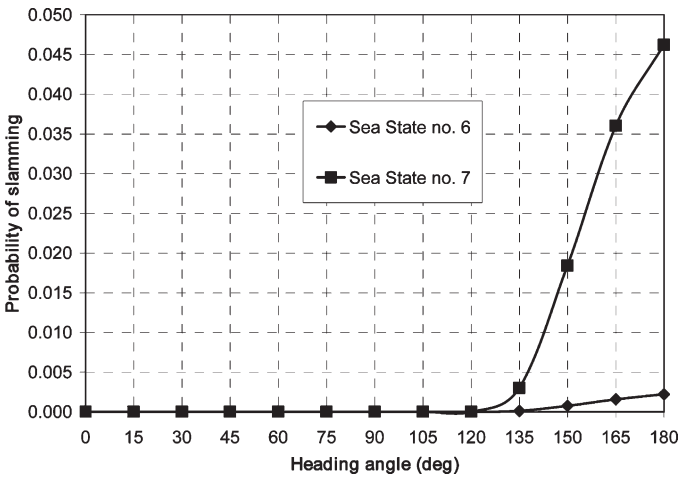

Fig. 5 Probability of slamming for S-175 as a function of ship relative heading angle and sea state

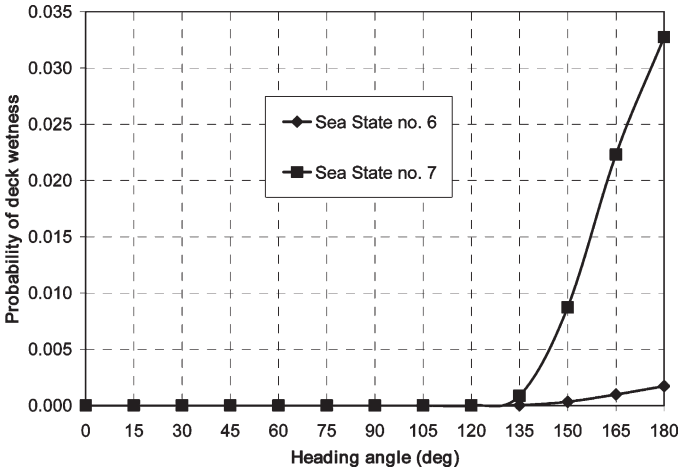

Fig. 6 Probability of deck wetness for S-175 as a function of ship relative heading angle and sea state

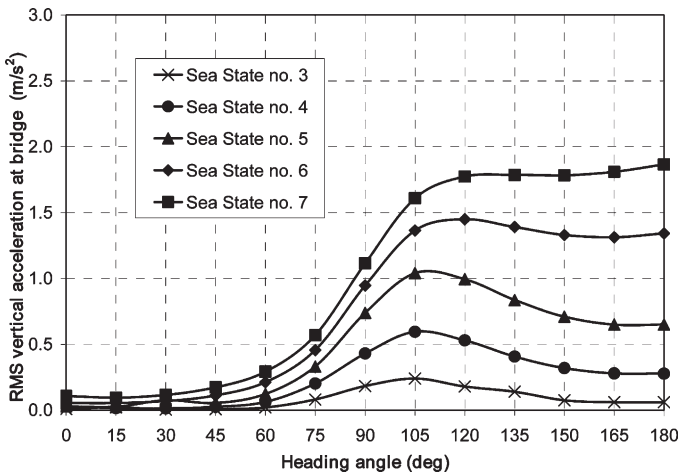

Fig. 7 RMS vertical acceleration at the bridge for S-175 as a function of ship relative heading angle and sea state

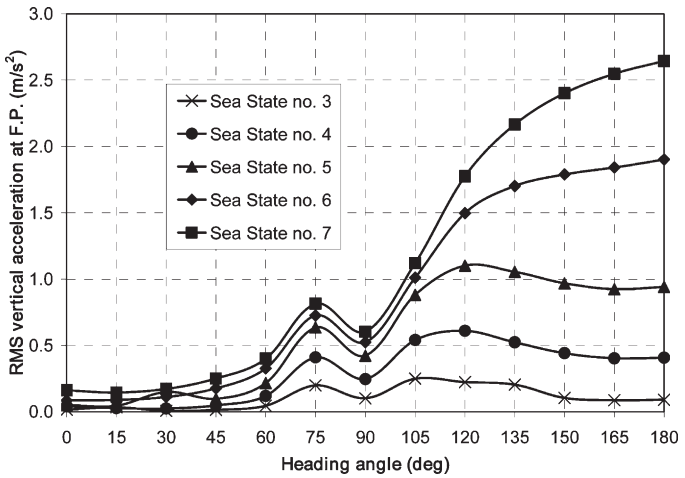

Fig. 8 RMS vertical acceleration at the F.P. for S-175 as a function of ship relative heading angle and sea state

4.1. Maximum mean attainable speed analysis

In Fig. 1, the computed maximum mean attainable speed is plotted as a function of relative heading angle for each given sea state. In order to perform a complete analysis of the speed data, speed values for intermediate heading angles were obtained through linear interpolation.

In this research, the vessel routes are assumed to not be long enough for the seaway to evolve from one sea state to another. Thus, the assumption is made that the sea state is a fixed parameter for any given trip. This optimal short-range routing is applicable to a wide range of applications, such as naval ships, coast guard patrols, recreational vessels, and tenders and refueling vessels servicing larger ships. It is also worth noting that since the maximum mean attainable vessel speed in a stationary seaway only depends on the heading and not on the vessel location or time, we can conclude that the seaway considered here is homogenous over space and time.

After analyzing the numerical maximum mean attainable speed results, it was concluded that no analytical function can adequately explain the variation of the speed data for Sea States 5 through 7. However, another approach to vessel speed data analysis was found to be more successful. Maximum attainable vessel speed polar plots for the S-175 numerical results, shown in Fig. 9, reveal a useful property of the speed functions. Specifically, the vessel polar plots for each sea state enclose a convex linear path attainable region.

For a given sea state, each maximum vessel speed polar plot bounds a region of the sea that a vessel can reach along a straight line path within one unit of time (1 hour for speed measured in knots) from the origin [point (0,0)]. We call such an area of the sea a *linear path attainable region* for point (0,0). These attainable regions for our numerical results of the maximum mean attainable speed for the S-175 are convex sets for all sea states (i.e., the line segment connecting any two points in the set is fully contained in that set). Proposition 1 below conveys the significance of the linear path attainable region convexity property.

Proposition 1. A fastest path from point *A* to point *B* is a path along the straight line connecting these two points if the set of all points that a vessel can travel to along a straight line within one unit of time is convex (i.e., if the linear path attainable region is convex).

Note that this might not be the only path corresponding to the minimum travel time between the two points, but rather there is no path for the convex linear path attainable region that is faster than straight line path *AB*. See the Appendix for a proof of Proposition 1.

Proposition 1 guarantees that the fastest travel path from the origin point *A* to the destination point *B* is the straight line segment *AB*. However, some of the traveling directions might not be feasible. In particular, the adopted seakeeping operability limiting criteria render some of these traveling directions infeasible. The fastest path according to Proposition 1 will not be feasible if the traveling direction *AB* violates at least one of these constraints. In that case, we need to seek an alternative route. In fact, if some of the ship headings are not feasible because of the adopted constraints, the *constrained linear path attainable region* (corresponding to those destinations that are *feasibly* reachable within one unit of time) will not be convex; thus, Proposition 1 will not be applicable.

Figures 10 to 12 illustrate the constrained linear path attainable regions for the S-175 in Sea States 5 through 7, respectively, taking into account all the operational constraints listed in Table 3. Thus, it is essential to understand how the fastest-path travel time changes if the linear path attainable region is no longer convex. A bound on the shortest travel time error will be derived assuming that a straight line path is implemented for a nonconvex attainable region situation.

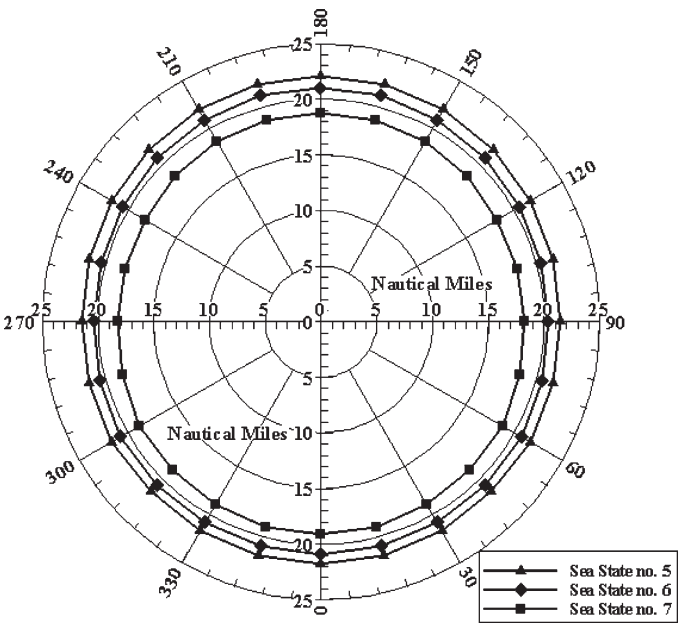

Fig. 9 Linear path attainable regions for S-175 for Sea States 5 through 7

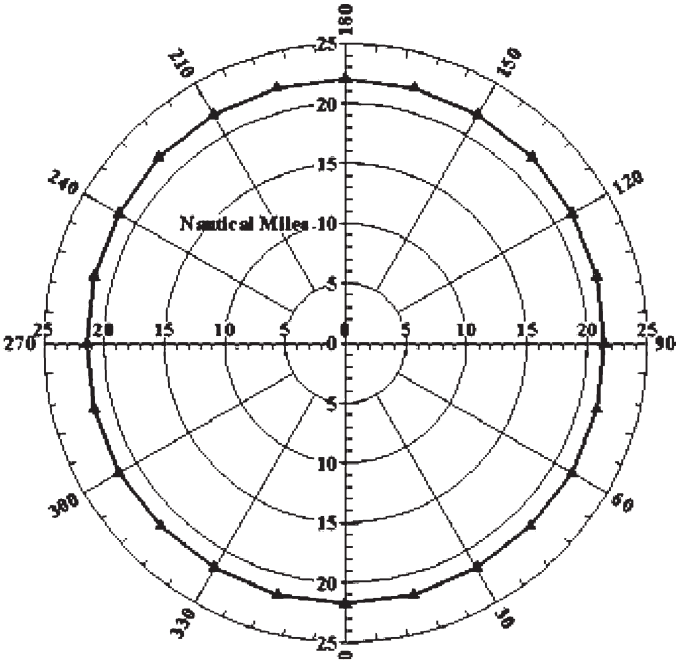

Fig. 10 Constrained linear path attainable regions for the S-175 for Sea State 5

4.2. Bound on the optimal travel time for a nonconvex linear path attainable region

Let S denote a linear path attainable region centered at point A, and suppose it is not convex. Then, a bound on the potential decrease in travel time from A to B can be derived by following the optimal (not necessarily linear) path instead of the straight line path. Consider S': = conv(S); that is, S' is the convex hull of set S, or S' is the smallest convex set that fully contains set S. Also, define K and K'. $K = AB \cap \text{bd}(S)$ and $K' = AB \cap \text{bd}(S')$, where bd($X$) denotes the boundary of a set X (see Fig. 13). Then, a bound on the optimal travel time, t^*, for a nonconvex attainable region can be derived:

$$\frac{d(AB)}{d(AK')} \le t_B \le \frac{d(AB)}{d(AK)} \tag{5}$$

$$\beta = \frac{d(AK)}{d(AK')} \le 1 \tag{6}$$

$$\beta t(AB) \le t^* \le t(AB) \tag{7}$$

where $t(AB)$ is the travel time along straight line path AB, $d(AB)$ is the distance between points A and B, and t_B is a nondimensional bound variable.

From equation (6) and inequality (7), we can conclude that the vessel travel time would decrease at most by $(1 - \beta)\cdot 100\%$ if the vessel follows an optimal path instead of traveling along the straight line path from A to B. This bound is especially important for finding the trade-off between time spent to find the optimal solution and improvement in the total travel time possible.

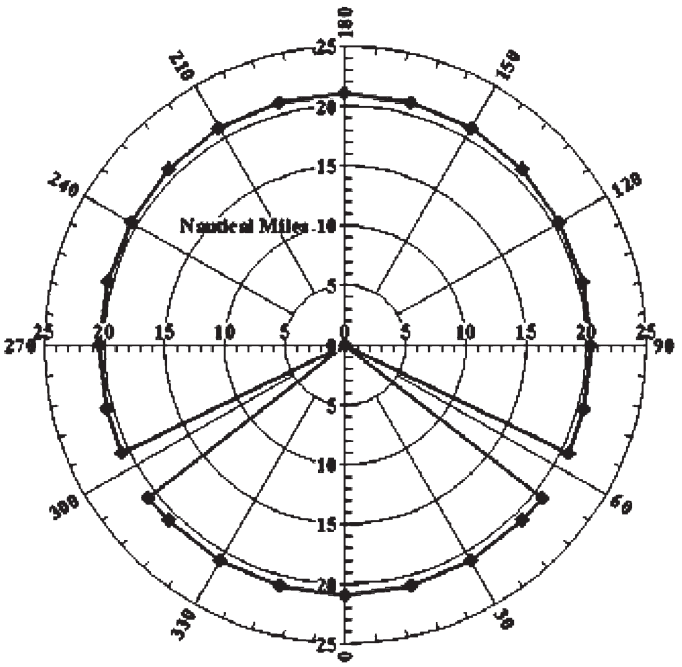

Fig. 11 Constrained linear path attainable regions for the S-175 for Sea State 6

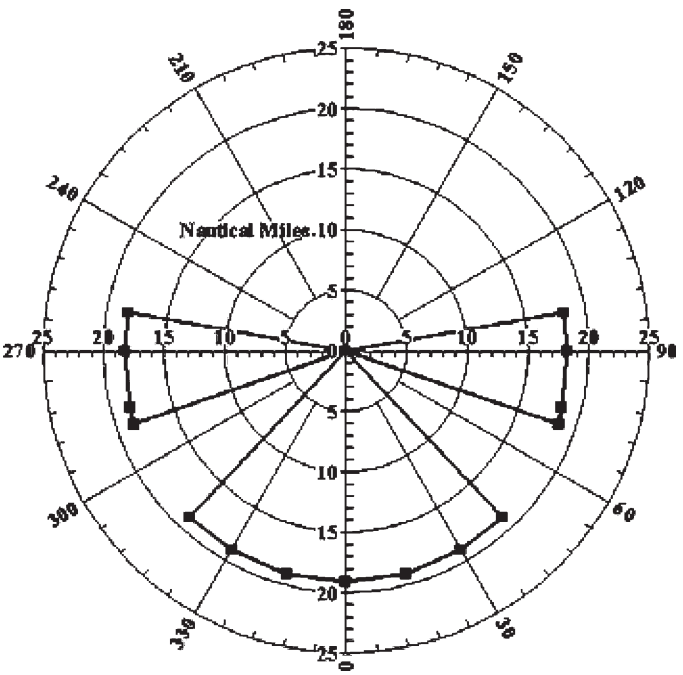

Fig. 12 Constrained linear path attainable regions for the S-175 for Sea State 7

4.3. Fastest path for a constrained linear path attainable region

The lower bound on the smallest travel time obtained in inequality (7) is also important in finding the optimal solution for the constrained fastest-path problem. It was noted earlier that added operational constraints introduce intervals of infeasible heading directions as shown for Sea States 6 and 7 in Figs. 11 and 12, respectively. Proposition 2 below provides one of several fastest paths from A to B, if the heading direction AB belongs to one of these infeasible heading intervals. To prove that the proposed path is in fact a fastest path, the travel time for this path is shown to be equal to the lower bound on travel time computed in equation (7).

Proposition 2. Suppose the heading direction of the path AB belongs to (θ_a, θ_b), where (θ_a, θ_b) is the interval of infeasible heading directions. Then, if the vessel unconstrained linear path attainable region is convex, a fastest path from point A to point B is a path ACB where AC has a heading angle θ_a and CB has an angle θ_b.

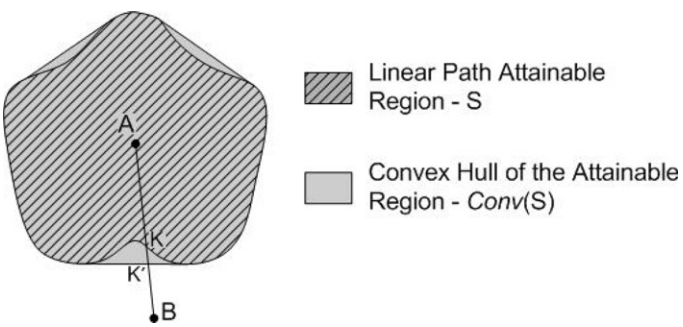

Fig. 13 Computing bound on an optimal travel time for nonconvex attainable region

Proof. Let $V(\theta)$ denote the vessel speed as a function of heading direction θ. Then, define points x and y as $x = A + [V(\theta_a) \cos(\theta_a - 90°), V(\theta_a) \sin(\theta_a - 90°)]$ and $y = A + [V(\theta_b) \cos(\theta_b - 90°), V(\theta_b) \sin(\theta_b - 90°)]$ (see Fig. 14). Note that points x and y lie on the boundary of the constrained linear path attainable region S centered at A. Hence, the travel time from A to either one of these points is equal to 1 unit of time. Recall that point K' is the intersection point of line segment AB and the boundary of the convex hull of S. Then, point K' can be expressed as $K' = \lambda x + (1 - \lambda)y$ for $0 \leq \lambda \leq 1$, since K' lies in the convex hull of set S. Note that point K' can be reached in one unit of time following the path $AC'K'$ where $C' = A + \lambda(A - x)$; that is, $AC' \parallel Ax$ and $C'K' \parallel Ay$. If the path $AC'K'$ is scaled up by a factor of $d(AB)/d(AK')$, path ACB is obtained with the total travel time $d(AB)/d(AK')$. Note that travel time for path ACB is equal to the lower bound on the optimal travel time in inequality (7). Hence, path ACB is an optimal path from A to B.

An alternative proof follows from the fact that triangle Axy is similar to triangle $C'xK'$ where the corresponding sides lengths ratio is equal to $(1 - \lambda)$.

This proposition implies that the fastest path would be to follow the direction of either one of the boundary heading angles, until the other boundary direction would deliver the vessel to the required destination. It needs to be mentioned that there are several paths with the minimum travel time. Figure 14 illustrates an application of Proposition 2 to find two of the fastest paths for Sea State 7 (both paths ACB and ADB have the minimum travel time).

Note that for the constrained linear path attainable region, the straight line path AB is still optimal if its heading direction is feasible. To show that this is true, observe that $\beta = 1$ in inequality (7) for this scenario; hence, travel time for a straight line path is equal to the lower bound on optimal travel time.

5. Discussion and conclusions

Proposition 2 establishes a fastest path from A to B to consist of two sequential line segments AC and CB, if heading AB belongs to an infeasible heading interval (θ_a, θ_b). Here, line segment AC has a heading angle θ_a, and CB has a heading angle θ_b. While ACB is proven to be an optimal path, in practice, an actual vessel is incapable of making a sudden heading change from θ_a to θ_b and hence cannot follow this fastest path. A control-feasible path from A to B would have to replace a sharp turn at point C by a smooth curve tangential to AC and CB (see Fig. 15).

However, if a vessel were to follow this smoothed path, the part of the path that deviates from ACB corresponds to infeasible headings that span the interval (θ_a, θ_b). Thus, this path could violate the active operability limiting criteria at these headings during the turn. To produce a path that violates neither vessel control system limitations nor operational constraints, a vessel is required to slowdown while making the turn. By reducing the nominal speed while traveling in the heading directions within the interval (θ_a, θ_b), the vessel motions are decreased, thus, making these headings feasible. This voluntary speed loss results in new attainable regions. For instance, attainable regions with

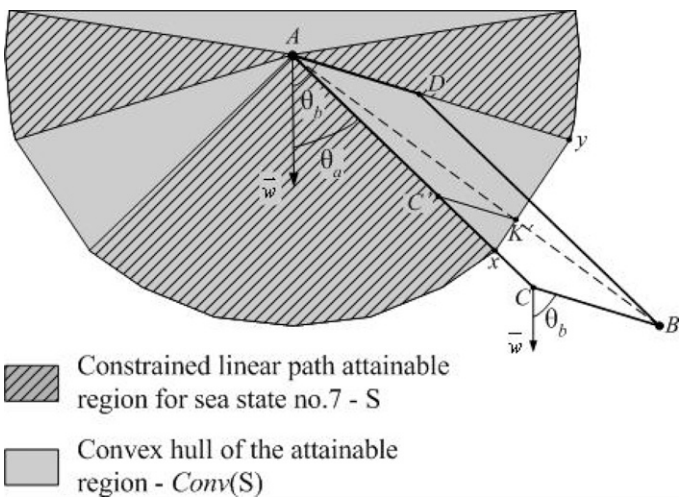

Fig. 14 Fastest paths from A to B are ACB and ADB

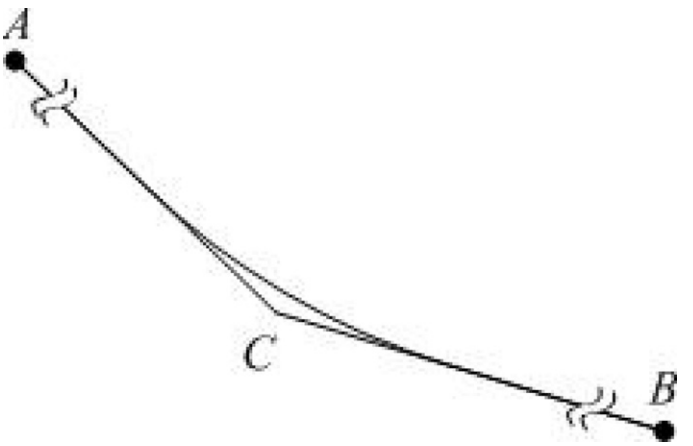

Fig. 15 Controls feasible path from A to B is a smooth curve

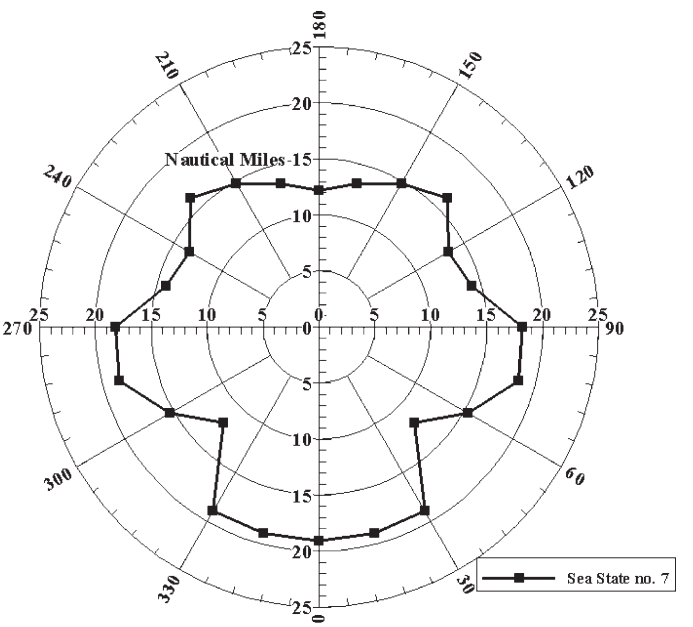

Fig. 16 An example of linear path attainable regions for the S-175 corresponding to voluntary speed loss at Sea State 7

voluntary speed loss for the S-175 for Sea State 7 are shown in Fig. 16. For most ship headings, the maximum mean attainable speed corresponds to the value required to avoid exceeding one of the operability limiting criteria rather than overcoming the added resistance.

While voluntary speed loss results in additional feasible headings, the new linear path attainable region often loses its convexity, which is a necessary condition for both Propositions 1 and 2. Hence, these propositions cannot be used to find a fastest path for attainable regions such as the one shown in Fig. 16. This conclusion leads to an interesting topic for future research: computation of the fastest path for a nonconvex linear path attainable region. For instance, the operational constraints considered here result in a set of infeasible headings. This situation corresponds to segment "cut-out" from otherwise convex attainable regions. Proposition 2 defines a fastest path for these cases. However, other constraints might result in more general modifications to the linear path attainable regions and also result in an arbitrary nonconvex set. Ongoing research will address this more wide-ranging case. In addition, relaxing time and/or space homogeneity of the sea domain as well as introducing stationary obstacles are other interesting extensions to explore.

While the presented analysis is restricted to finding a path that minimizes the total travel time, the same results are valid for other path-optimizing problems. In the case of a fastest-path problem, the linear path attainable region is defined to be the set of points a vessel can travel to in a single unit of time. Likewise, the problem of finding a path minimizing the fuel consumption of a vessel can be addressed by redefining the linear path attainable region to be a set of points a vessel can travel to while consuming a single unit of fuel. Thus, the results simply translate to other optimization problems and a wide area of applications.

Acknowledgment

This paper is the result of work sponsored by the Office of Naval Research through the Multidisciplinary University Research Initiative (MURI) Optimum Vessel Performance in Evolving Nonlinear Wave Fields under contract N00014-05-1-0537. This support is gratefully acknowledged.

References

BECK, R. F., TROESCH, A. W., AND HE, H. 2004 *Documentation and User's Manual for the Computer Program SEAKEEPER.NTD,* Formation Design Systems Pty, Fremantle, WA, Australia.

FAULKNER, F. D. 1963 Numerical methods for determining optimal ship routes, *Journal of the Institute of Navigation,* **10,** 4, 351–367.

FDS 2006a *Seakeeper Windows Version 12 User's Manual,* Formation Design Systems Pty, Fremantle, WA, Australia.

FDS 2006b *Maxsurf Windows Version 12 User's Manual,* Formation Design Systems Pty, Fremantle, WA, Australia.

FDS 2006c *Hullspeed Windows Version 12 User's Manual,* Formation Design Systems Pty, Fremantle, WA, Australia.

FRANK, W. 1967 *On the Oscillation of Cylinders in or Below the Free Surface of Deep Fluids,* Hydrodynamics Laboratory, Naval Ship R&D Center, Technical Note 69.

FUJII, H., AND TAKAHASHI, T. 1975 Experimental study on the resistance increase of a ship in regular oblique waves, *Proceedings,* 14th ITTC, International Towing and Tank Conference, National Research Council of Canada, September, Ottawa, Ontario, Canada, 351–359.

GERRITSMA, J., AND BEUKELMAN, W. 1964 The distribution of hydrodynamic forces on a heaving and pitched ship model in still water, *International Shipbuilding Progress,* **11,** 506–522.

GERRITSMA, J., AND BEUKELMAN, W. 1972 Analysis of the resistance increase in waves of a fast cargo ship, *International Shipbuilding Progress,* **19,** 285–293.

HOLTROP, J. 1984 A statistical re-analysis of resistance and propulsion data, *International Shipbuilding Progress,* **31,** 363, 272–276.

ITTC 1987 S-175 comparative model experiments—Report of the Seakeeping Committee, *Proceedings,* 18th ITTC, International Towing Tank Conference, The Society of Naval Architects of Japan, October, Kobe, Japan, 415–427.

LEE, W. T., BALES, W. L., AND SOWBY, S. E. 1985 *Standardized Wind and Wave Environments for North Pacific Ocean Areas,* DTNSRDC, Washington, DC, R/SPD-0919-02.

LIN, W. C., AND REED, A. M. 1976 The second order steady force and moment on a ship moving in an oblique seaway, *Proceedings,* 11th Symposium on Naval Hydrodynamics, London, Great Britain, 333–351.

MARUO, H. 1957 The excess resistance of a ship in rough seas, *International Shipbuilding Progress,* **4,** 337–345.

MITCHELL, J. S. B., AND PAPADIMITRIOU, C. H. 1991 The weighted region problem: finding shortest paths, *Journal of the Association for Computing Machinery,* **38,** 1, 18–73.

NAKAMURA, S. 1976 Added resistance and propulsive performance of ships in waves, *Proceedings,* International Seminar on Wave Resistance, Tokyo, Japan, The Society of Naval Architects of Japan.

NORDFORSK. 1987 The Nordic Cooperative Project, Seakeeping Performance of Ships, *Assessment of a Ship Performance in a Seaway,* MARINTEK, Trondheim, Norway.

OCHI, M. K., AND MOTTER, L. E. 1973 Prediction of slamming characteristics and hull responses for ship design, *Transactions SNAME,* **81,** 144–176.

PAPADAKIS, N. A., AND PERAKIS, A. N. 1990 Deterministic minimal time vessel routing, *Operations Research,* **38,** 426–438.

PHILPOTT, A. B., SULLIVAN, R. M., AND JACKSON, P. S. 1993 Yacht velocity prediction using mathematical programming, *European Journal of Operational Research,* **67,** 13–24.

SALVESEN, N., TUCK, E. O., AND FALTINSEN, O. 1970 Ship motions and sea loads, *Transactions SNAME,* **78,** 250–287.

SALVESEN, N. 1978 Added resistance of ships in waves, *Journal of Hydronautics,* **12,** 1, 24–34.

ST. DENIS, M., AND PIERSON, W. J. 1953 On the motions of ships in confused seas, *Transactions SNAME,* **61,** 280–357.

STROM-TEJSEN, J., YEN, H. Y. H., AND MORAN, D. D. 1973 Added resistance in waves, *Transactions SNAME,* **81,** 109–143.

Appendix: Proof of Proposition 1

Proposition 1. A fastest path from point A to point B is a path along the straight line connecting these two points if the set of points that a vessel can travel to along a straight line within one unit of time (linear path attainable region) is convex.

Proof. Let $S_{(x,y,a)}$ be a set of points that a vessel can travel to along a straight line path within a units of time from point (x,y). $S_{(x,y,1)}$ is the linear path attainable region discussed earlier. Since convexity of $S_{(x,y,1)}$ implies that set $S_{(x,y,a)}$ is convex, and vice versa, we need to show that if $S_{(x,y,a)}$ is convex, a fastest path from point A to point B is a path along the straight line AB.

Path traveled by a vessel along any rectifiable curve from A to B can be approximated by a set of straight line segments, such that segments ends lie on the curve. As the number of segments approaches infinity, the length of the curve approaches the sum of straight line segments lengths (see Fig. A1). Thus, to show that the path along straight line AB is a fastest path from A to B, we need to show that traveling between any two points, call them A' and B', is never faster along path $A'HB'$ for an arbitrary H than along the straight line $A'B'$.

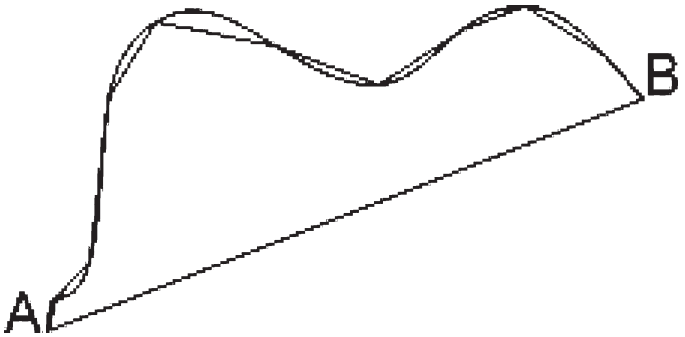

Fig. A1 Curve path approximation

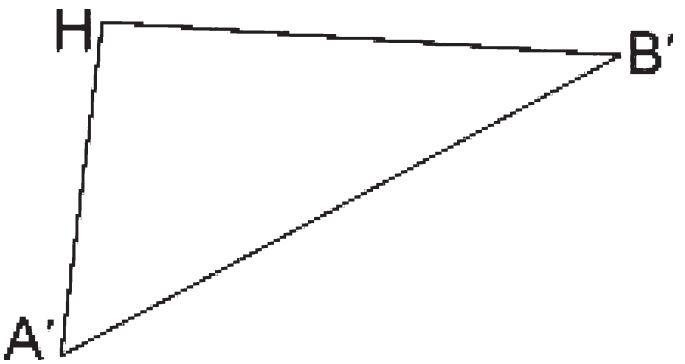

Fig. A2 To show $t(A'B') \leq t(A'HB')$

Select an arbitrary point H that does not lie on the line connecting A' and B'. We show that traveling time along straight path $A'B'$, written as $t(A'B')$, is never greater than traveling time along path $A'HB'$, $t(A'HB')$ (Fig. A2). Note that since vessel speed only depends on the heading angle, using the traveling time additive property we can conclude that $t(A'HB') = t(A'H) + t(HB')$.

Hence, we need to show that $t(A'B') \leq t(A'HB')$:

1. Let $t(A'H) = a$, find C that lies on line $l_{A'B'}$ such that $t(A'C) = a$, where $l_{A'B'}$ is the line connecting A' and B'. For any two points $P = (x_P, y_P)$ and $Q = (x_Q, y_Q)$ we define distance $d(P,Q)$ as:

$$d(P,Q) = \sqrt{(x_P - x_Q)^2 + (y_P - y_Q)^2} \qquad \text{(A1)}$$

   Since the vessel speed only depends on the heading angle, from the traveling time proportionality property we can conclude that if $d(A',C) \geq d(A',B')$, then $t(A'B') \leq a \rightarrow t(A'B') \leq t(A'H) \leq t(A'HB')$ and the proposition is proven.
2. Assume $d(A',C) < d(A',B')$. We know that for any nonempty convex set X and any x_0 lying on the boundary of set X, there exists a supporting hyperplane to X at x_0. Given that $S_{(A',a)}$ is convex, we can find its supporting hyperplane at point C, call it Φ_C. Since H belongs to $S_{(A',a)}$, H also belongs to the same half-space as A'.
3. Let $E = \Phi_C \cap HB'$ (see Fig. A3). Note that in the extreme scenario H lies on Φ_C, then $E = H$.

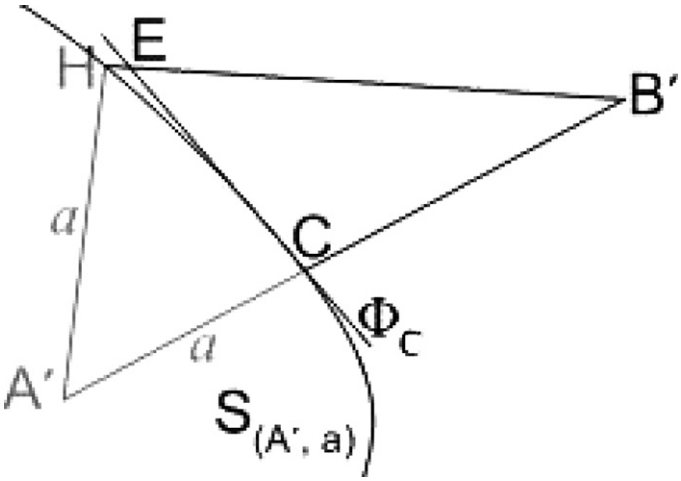

Fig. A3 Supporting hyperplane Φ_C

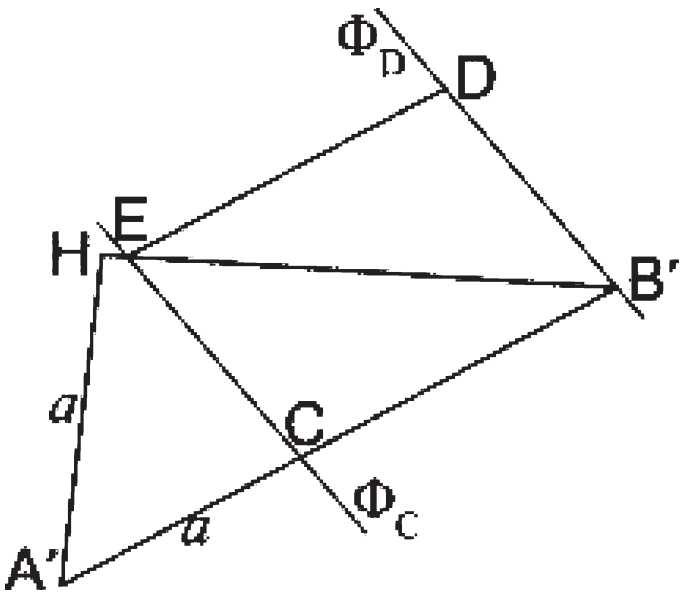

Fig. A4 Traveling time $t(CB') = t(ED)$

4. Find D such that $ED \parallel CB'$, and D lies in the same half-space as B' relative to the hyperplane Φ_C. Given that vessel speed only depends on the heading angle, we know that traveling time along any given vector is independent of the vector location. Thus, $t(CB') = t(ED)$ (see Fig. A4).
5. Let Φ_D be the supporting hyperplane to $S_{[E,\ t(ED)]}$ at point D, which is parallel to Φ_C. Then, B' lies on Φ_D and $t(EB') \geq t(ED)$. From that and the fact that vessel speed is time and space homogeneous we obtain that $t(HB') \geq t(EB') \geq t(ED) = t(CB')$.
6. But then $t(A'B') = t(A'C) + t(CB') = a + t(CB') = t(A'H) + t(CB') \leq t(A'H) + t(HB') = t(A'HB')$.